Architecture and Performance Evaluation of Bundled-path-routing Multi-band Optical Networks

Ryuji Munakata[1], Takuma Kuno[1], Yojiro Mori[1], Shih-Chun Lin[2], Motoharu Matsuura[3], Suresh Subramaniam[4], Hiroshi Hasegawa[1]

[1]Nagoya University, Furo-cho, Chikusa-ku, Nagoya, 464-8603 Japan
[2] North Carolina State University, Raleigh, NC 27695 USA
[3] University of Electro-communications, 1-5-1 Chofugaoka, Chofu, Tokyo, 182-8585 Japan
[4] George Washington University, 800, 22nd St. NW, Washington DC, 20052 USA
munakata.ryuji.m4@s.mail.nagoya-u.ac.jp

Abstract: We propose a novel bundled-path-routing node architecture for multi-band optical networks and a network design algorithm based on graph degeneration. Feasibility is demonstrated through experiments on a prototype with 300.8 Tbps throughput. © 2023 The Authors

1. Introduction

Rapid traffic growth in the Internet and the saturation of single-mode fiber (SMF) capacity enhancement motivate the development of transmission technologies that realize higher spatial parallelism and wider frequency bandwidth [1,2]. Space-division multiplexing using multi-core/multi-mode fibers or multiple SMFs laid in parallel on each link can substantially increase the network capacity [3,4]. Multi-band transmission enables us to utilize unused frequency bands such as the S&L-bands to supplement the C-band [5,6]; the broadened frequency bandwidth will more than double the capacity of SMFs. We have to well utilize such novel transmission technologies to cope with the relentless and exponential traffic growth.

Optical cross-connects (OXCs) placed at nodes bridge the fibers/cores connected to the nodes. An OXC generally consists of wavelength selective switches (WSSs) which are located at input and/or output ports of the OXC. WSS degree must equal or exceed that of the OXC; if WSS degree is insufficient, then multiple WSSs must be cascaded to fulfill the degree requirement. However, the number of WSSs in a node increases in square order of OXC degree and more erbium-doped fiber amplifiers (EDFAs) are necessary to compensate for the accumulated transmission loss at cascaded WSSs [7]. Furthermore, massive fiber inter-connections between all input and output port pairs of the OXC are mandatory. The introduction of multi-band transmission necessitates the use of multiple OXCs dedicated to different bands, and we need WSSs tailored to these bands; e.g., the use of three OXCs for S/C/L-bands triples the number of WSSs. On the other hand, large-scale optical matrix switches are now attracting attention due to their scalability, over 300×300, and lower transmission loss [8-10]. Moreover, optical switches can route optical paths in different frequency bands. Thus, large-scale matrix switches can be scalable and cost-effective routing devices for multi-band optical networks.

In this paper, we propose a novel optical node architecture for multi-band optical networks that adopts two-stage path routing; bundling of optical paths distributed to multiple frequency bands and switching of bundled paths. For each input port, a set of small-port-count WSSs for different frequency bands are used as dynamic optical filters to form a small number of path groups named flexible wavebands. Paths in a flexible waveband can distribute all frequency bands. Paths in a flexible waveband are routed together by a large-scale optical matrix switch and wavebands are multiplexed at output ports. The number of and the degree of necessary WSSs are substantially reduced with the use of two-stage path routing. A graph degeneration based network design algorithm is developed to support the routing scheme. Numerical simulations elucidate that the routing performance deterioration relative to conventional WSS-based nodes, which need many high-port-count WSSs and thus are hard to realize, does not exceed 2% in high-traffic-intensity cases. Transmission experiments with a 16×16 prototype show that 188-wavelength 32 Gbaud DP-4QAM signals aligned on 50 GHz spaced grids in the C/L-bands can traverse 25 (C-band)/23 (L-band) nodes, where the distance between nodes is 100 km. The total throughput of the prototype reaches 300.8 Tbps.

2. Proposed Multi-band Flexible-waveband-routing Node Architecture

We assume fully transparent optical networks that adopt multi-band transmission; e.g., the S&L-bands are used in addition to the conventional C-band. Figure 1(a) shows an extended version of conventional WSS-based OXC node that realizes multi-band transmission; multiple OXCs dedicated to different frequency bands are used in parallel and bridged by WDM couplers. Considering the scalability issue of conventional OXCs, we have proposed an alternative architecture named flexible-waveband-routing node such that optical paths are bundled with WSSs at the input side, as flexible wavebands, and then the wavebands are routed with delivery-and-coupling (DC) switches (Fig.

1(b)) [11]. As the number of wavebands B can be small (2-4), cost-effective small-port-count WSSs can be used. No multi-band extension of flexible-waveband-routing has been studied so far. The drawback of flexible-waveband-routing nodes is that the signal power loss at the DC switches is severe, and hence, the scalability of nodes and transparent transmissible distance is quite limited.

The introduction of multi-band transmission to flexible-waveband-routing is possible by replacing a C-band WSS by a set of multiple WSSs dedicated to different frequency bands. In order to resolve the severe power loss issue faced by flexible-waveband-routing nodes, we propose to use optical matrix switches for bundled-path-routing (Fig. 1(b)). Different from the original DC-switch based architecture, multiple wavebands from different input fibers cannot be multiplexed at the matrix switch. However, the following network design algorithm makes the novel architecture sufficiently efficient with regard to path routing.

<Design of Flexible-waveband-routing Networks by Iterative Degeneration of Intra-node Interconnection >

For given topology and path setup demands, conduct a static design of an initial fiber network with conventional nodes. Define a full-mesh graph representing the switching status of each node and assign the same positive weighting value to all intra-node links. Increase the weighing values of intra-node links which are not traversed by a sufficient number of paths. Remove and accommodate all paths according to the minimum weight routing. Iterate this procedure and terminate if the number of links traversed by optical paths for each input becomes equal to or less than B. If the termination condition is still violated, after sufficient number of iterations, at some input, then install new fibers to resolve the violation and terminate.

The proposed routing scheme can also be realized by interchanging optical couplers/WSSs at the input/output sides in Fig. 1(b); i.e., the broadcast-and-select architecture. The detailed broadcast-and-select node architecture for multi-band transmission is shown in Fig. 1(c).

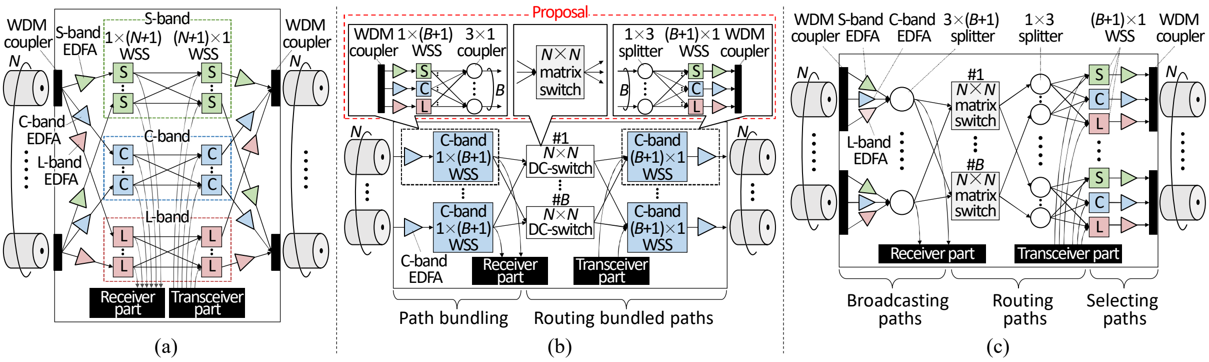

Fig. 1. Node architectures: (a) Typical WSS-based node for multi-band transmission; (b) Flexible-waveband-routing node and highlight of the novel parts for multi-band transmission; (c) The proposed broadcast-and-select node for multi-band transmission.

3. Numerical Simulations

The topologies tested are a 4×4 regular-mesh network, Kanto (Tokyo metropolitan) network, and US-metro network as shown in Fig. 2. The available frequency range of each fiber is set to 9.6 THz over multiple bands; i.e., 768 12.5 GHz frequency slots are employed. Traffic demands are generated as a set of optical path establishment requests, where the source and destination nodes are randomly and uniformly distributed. We parameterize the traffic intensity represented as the average number of optical paths between each node pair. The use of three types of optical paths is assumed; 100 Gbps, 400 Gbps, and 1 Tbps that occupy 4, 7, and 15 slots, respectively. The path-occurrence probability is set to 1/3. We employ the routing performance of the conventional WSS-base node as the baseline. This node can route any input optical wavelength to any output port. The results are the averages of 20 calculations in each plot.

Network topology	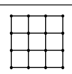 (a) 4×4 regular-mesh	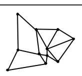 (b) Kanto	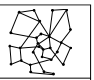 (c) US-metro
# of nodes	16	11	29
# of links	24	18	41
Max. node degree	4	5	7
Ave. node degree	3	3.27	2.83

Fig. 2. Tested network topologies.

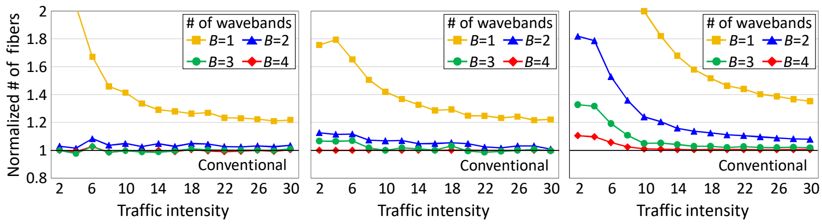

Fig. 3. The normalized number of necessary fibers relative to conventional WSS-based node. (a) 4×4 regular-mesh network, (b) Kanto network, and (c) US-metro network.

Figure 3 shows the number of necessary fibers versus traffic intensity. When the traffic intensity is small, the increase in the number of fibers is large. This is because the number of accessible adjacent nodes is smaller if the number of fibers connected to nodes is small. When the number of wavebands B is set to 2, the fiber increment at high-traffic-intensity is less than 8% for all topologies. The gap against the conventional WSS-based node decreases as B increases. The fiber increment penalty at the high-traffic-intensity examined is less than 2% for all network topologies if B is set to 3. The penalty is negligible if B is set to 4.

4. Transmission Experiments

To verify the feasibility of our proposed node architecture, we conducted a transmission experiment. Figure 4 illustrates the experimental configuration. The adopted node configuration is that in Fig. 1(c). This proof-of-concept experiment omitted the S-band due to the available devices. A 32 Gbaud 4QAM signal was created by an IQ modulator (IQM) driven by an arbitrary-waveform generator (AWG). After that, the DP-4QAM signal was emulated in a split-delay-combine manner. As non-target signals, 188-wavelength 32 Gbaud DP-4QAM signals were generated using 188 continuous waves (CWs), where 96-wavelength signals and 92-wavelength signals were aligned on the 50 GHz grid in the C-band and L-band, respectively. The power of the non-target signals was flattened by gain-flattening filters (GFFs) and adjusted by variable optical attenuators (VOAs) and EDFAs. The target signal and the non-target signals were merged at 4×1 WSSs and a WDM coupler yielding 188 channels of 32 Gbaud DP-4QAM signal. The signals entered a recirculating fiber loop consisting of a 2×2 optical splitter, a 100 km SMF, the OXC under test, a VOA, and two synthesized switches (SWs). The OXC consisted of a WDM coupler, a C-band EDFA, an L-band EDFA, a 2×4 splitter, a 16×16 optical selector (OS), a 1×2 splitter, a C-band 4×1 WSS, an L-band 4×1 WSS, a C-band EDFA, an L-band EDFA, and a WDM coupler. Here, we added intra-band and inter-band crosstalk assuming the practical systems. After looping multiple times, the signals entered a 100 km SMF. Finally, the signals were dropped by a 2×4 splitter, an optical tunable filter (TF), and a coherent receiver.

Figure 5 plots the BER versus hop count in the C-band and L-band transmission. The acceptable BER was set to 10^{-2} as we assume the use of forward error correction (FEC). We observed that the C-band and L-band signals can be transmitted 25 hops/2500 km and 23 hops/2300 km, respectively. The difference between the C-band and L-band mainly originated from the performance of our available EDFAs. These results clearly show that the proposed node can be applied to most metro networks. The total throughput of this prototype reaches 300.8 Tbps.

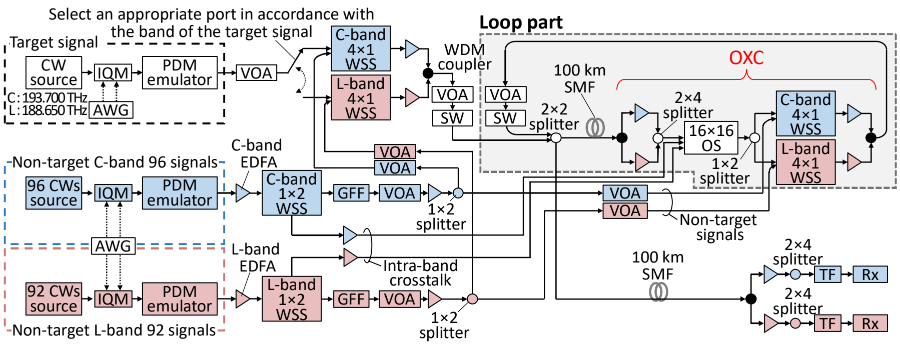

Fig. 4. Experimental configuration.

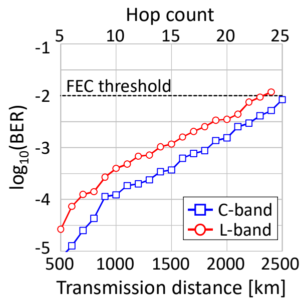

Fig. 5. Measured BERs versus hop count or transmission distance.

5. Conclusion

We proposed a novel bundled-path-routing node architecture for multi-band optical networks and developed a network design algorithm based on graph degeneration. Network simulations showed that the routing penalty will not exceed 2% relative to conventional nodes for high-traffic-intensity cases. A C+L-band 16×16 node prototype was tested to verify the feasibility of the proposed node architecture. The total throughput of the node reached 300.8 Tbps and we successfully realized transmission over 25 hops/2500 km (C-band) and 23 hops/2300 km (L-band). The proposed node is highly scalable because the node loss is virtually independent of the OXC degree.

Acknowledgments: This work was partly supported by NICT and NSF.

6. References

[1] Cisco Systems, Inc., White paper (2019).
[2] P. J. Winzer, Optica Opt. Photon. News **26**, 28-35 (2015).
[3] Y. Awaji, IEICE Trans. Commun. **E102-B**, 1-16 (2019).
[4] R. Luis *et al.*, ECOC, Th3C.5 (2022).
[5] A. Ferrari *et al.*, IEEE/Optica J. Lightw. Technol. **38**, 4279-4291 (2020).
[6] R. Sadeghi *et al.*, ECOC, We1B.2 (2022).
[7] M. Niwa *et al.*, IEEE/Optica J. Opt. Commun. Netw. **9**, A18-A-25 (2017).
[8] M. Ganbold *et al.*, IEICE Trans. Commun. **E103-B**, 679-689 (2020).
[9] M. Jinno *et al.*, IEEE/Optica J. Opt. Commun. Netw. **13**, A124-A134 (2021).
[10] T. Matsuo *et al.*, OFC, W3F.6 (2022).
[11] H. Hasegawa *et al.*, IEEE/Optica J. Opt. Commun. Netw. **8**, 734-744 (2016).